

Resonance frequencies of AlN and metal freestanding multilayers studied by picosecond ultrasonics

ピコ秒超音波法を用いた AlN/金属多層自立膜の共振周波数計測

Akira Nagakubo^{1†}, Tokihiro Nishihara², Hirotsugu Ogi¹ (¹Osaka Univ.; ²Taiyo Yuden Co. Ltd.)

長久保 白^{1†}、西原 時弘²、荻 博次¹ (1 阪大院工 2 太陽誘電株式会社)

1. Introduction

With the progress of wireless communication, filter devices have been keenly studied, and many acoustic filters, such as surface-acoustic-wave (SAW) filters and bulk-acoustic-wave (BAW) filters, are mounted in mobile phones. These filters are required to operate at high frequencies, with high temperature stability, broad and tunable band, and low energy loss. Communication frequency and the band width of SAW filters can be controlled by the pattern and alignment of the interdigital transducers. It is, however, difficult to make the operation frequency much higher (> 10 GHz).

On the other hand, the frequency of BAW filters is principally inversely proportional to the film thickness, allowing us to make higher-frequency filters. One of problems for BAW filters is energy loss: BAW filters use deposited piezoelectric thin films, whose vibration energy can easily propagate into adjacent layers. To reduce the energy leakage, the piezoelectric thin film is deposited on a Bragg reflector, which has a multilayer structure consisting of alternate high and low acoustic impedance materials with the quarter-wavelength thickness.

Another way to enhance the quality factor of a BAW filter is to make an air gap between the resonator and the substrate. The energy leakage of such a device can be significantly smaller than that of the Bragg reflector. Moreover, such an ideal resonator enables us to accurately measure acoustic properties of the films: As the operation frequency increases, sound attenuation becomes large, therefore, device designs become more important and difficult because the wavelength and film thickness decrease. Thin films usually exhibit different acoustic properties from bulk states, which depends on their thickness and deposition conditions^[2,3] especially in a thicker region. We have to design, for example, the film thicknesses of a Bragg reflector as quarter wavelength, which needs the accurate values of sound velocities for each layer for various film thicknesses. Therefore, high-frequency operations require us to evaluate the acoustic properties of every layer. Resonance frequencies of a self-standing film largely reflect

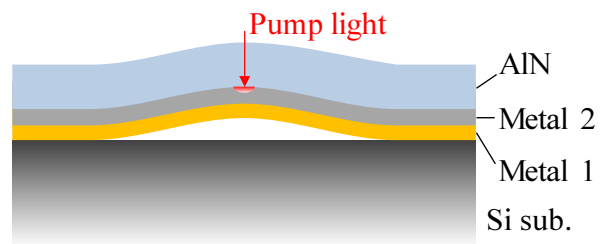


Fig. 1 Schematic of a dome-shape AlN BAW filter.

acoustic properties of every layer, allowing us to accurately determine acoustic properties of each layer. However, it is difficult to make and measure such an air gap resonator at ultrahigh frequencies. Because the self-standing area is confined to be $< \sim 1$ mm², a localized measurement within the area is needed.

In this study, we fabricated dome-shape AlN resonators with metallic electrodes with air gaps as shown in **Fig. 1** and measured their eigen-vibration modes in time domain using picosecond ultrasonics^[4,5]. We observed a dozen resonant modes, whose frequencies are up to around 60 GHz.

2. Experiment

We used two femtosecond titanium/sapphire pulse lasers to excite and detect the tens of GHz vibrations^[6]. The wavelength and repetition rate of the pulse light are 800 nm and 80 MHz, respectively.

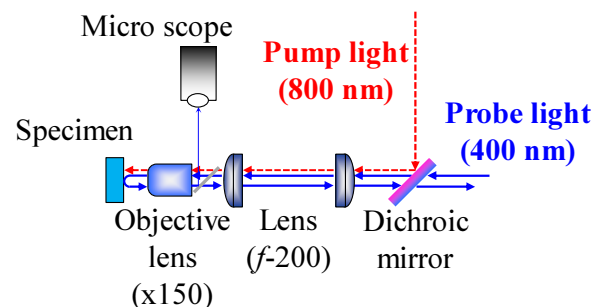


Fig. 2 Schematic of the optics around specimen. The pump and probe lights pass the same path after the dichroic mirror and normally enter the specimen. We used an objective lens of 150 magnification to focus the lights within the self-standing area.

The two lasers were synchronized within 150 fs jitter, and we can arbitrarily change the initial delay time of the two lasers with keeping the optics as the same setup.

During measurement, the light path of the pump light was mechanically shortened by using corner reflectors and a stepping motor to control the delay time of probe light pulses. We modulated the pump light as 100 kHz by using an acoustic optical modulator to enhance the signal-to-noise ratio, and used the first-order diffracted light. As shown in **Fig. 2**, the pump light pulse reflected at the dichroic mirror and entered a specimen through a 150-magnification objective lens. The spot diameter of the pump light was about 1 μm at the specimen surface. The metal layer absorbed the pump light pulse, which excited strain pulse and eigen vibrations of the self-standing film.

The excited vibration was detected by the time-delayed probe light pulse. The wavelength of the probe light was converted into 400 nm to separate the pump and probe lights by using a pair of plano-convex lens and a second harmonic generator of $\beta\text{-BaB}_2\text{O}_4$. Before the dichroic mirror, some of the probe light entered one of a photo diode of a balance

detector. 400-nm probe light transmitted the dichroic mirror and entered the specimen through the same path as the pump light. Reflected probe light from the specimen entered the other photo diode of the balance detector, and the power difference of the two diodes was outputted to a lock-in amplifier.

We inserted a variable attenuator before the objective lens to observe the specimen surface by a microscope, which enables us to exactly measure the acoustic properties of the self-standing area.

3. Results

Figure 3 (a) shows an observed vibration of the film. Only just after the thermal excitation, about 100-GHz oscillation appears (20–180 ps). This is a Brillouin oscillation of $\text{AlN}^{[7]}$. The half and end of the period, reflectivity largely changes (at ~ 100 and ~ 180 ps). At these time, the initial excited strain pulse at an AlN/metal boundary reaches at the AlN top surface and the AlN/metal boundary, respectively. After that, much “lower-frequency” (3–60 GHz) and large-amplitude oscillations appear. These oscillations are the eigen-vibration modes of the self-standing film, whose fast Fourier transformation (FFT) spectrum is shown in **Fig. 3 (b)**.

We will calculate the eigen frequencies by using a 1D plane wave propagation model, and inversely determine the elastic constants of each film at the same time. This method allows us to determine the acoustic properties of all layers.

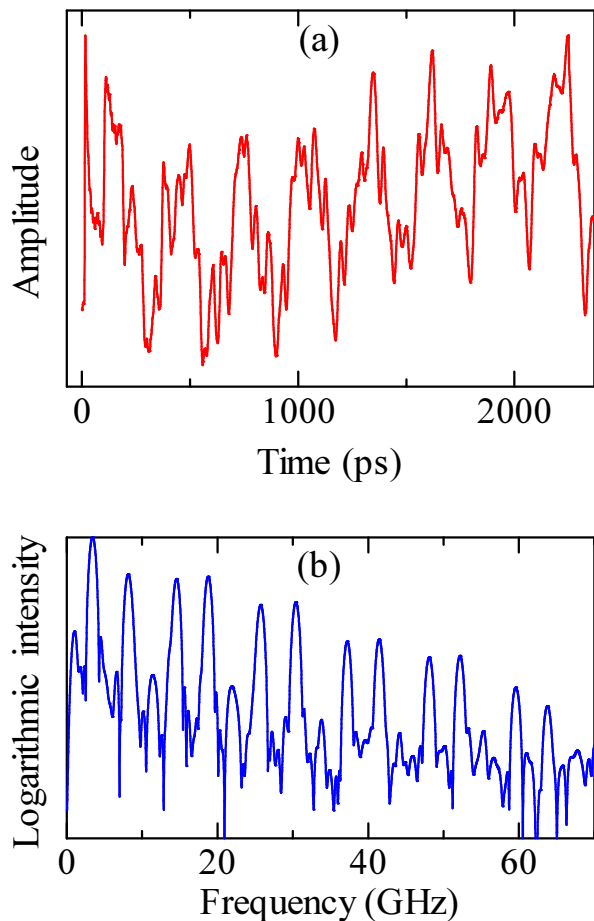


Fig. 3 (a) Observed vibration of the film and (b) corresponding FFT spectrum.

References

1. D. H. Kim, M. Yim, D. Chai, J. S. Park, and G. Yoon, *Jpn. J. Appl. Phys.* **43** (2004) 1545.
2. H. Ogi, M. Fujii, N. Nakamura, T. Yasui, and M. Hirao, *Phys. Rev. Lett.* **98** (2007) 195503.
3. H. Ogi, T. Shagawa, N. Nakamura, M. Hirao, H. Odaka, and N. Kihara, *Phys. Rev. B* **78** (2008) 134204.
4. C. Thomsen, J. Strait, Z. Vardeny, H. J. Maris, and J. Tauc, *Phys. Rev. Lett.* **53** (1984) 989.
5. C. Thomsen, H. T. Grahn, H. J. Maris, and J. Tauc, *Phys. Rev. B* **34** (1986) 4129.
6. K. Tanigaki, H. Ogi, H. Sumiya, K. Kusakabe, N. Nakamura, M. Hirao, and H. Ledbetter, *Nat. Commun.* **4** (2013) 2343.
7. A. Nagakubo, M. Arita, T. Yokoyama, S. Matsuda, M. Ueda, H. Ogi, and M. Hirao, *Jpn. J. Appl. Phys.* **54** (2015) 07HD01.